Proceedings of the 42th "Jaszowiec" International School and Conference on the Physics of Semiconductors, Wisła 2013

Effect of High Energy Electron Irradiation on Structure and Optical Properties of ZnO Films

D.V. Myroniuk[a,*], G.V. Lashkarev[a], I.I. Shtepliuk[a], V.Y. Lazorenko[a], V.T. Maslyuk[b], I.I. Timofeeva[a], A.S. Romaniuk[c], V.V. Strelchuk[c], O.F. Kolomys[c] and V.V. Khomyak[d]

[a]Frantsevich Institute for Problems of Material Science, NAS of Ukraine, 3 Krzhizhanivsky Str., 03680 Kyiv, Ukraine

[b]Institute of Electron Physics, NAS of Ukraine, 21 Universitetska Str., 88017 Uzhgorod, Ukraine

[c]Lashkaryov Institute of Semiconductor Physics, NAS of Ukraine, 41 pr. Nauki, 03028 Kyiv, Ukraine

[d]Fedkovich Chernivtsi National University, 2 Kotsubinsky Str., 58012 Chernivtsi, Ukraine

Zinc oxide films were grown on sapphire substrates by direct current magnetron sputtering and irradiated by electrons with energy 10 MeV and fluences 10^{16} and 2×10^{16} cm^{-2}. As-grown and irradiated samples were investigated by X-ray diffraction and photoluminescence spectroscopy. It was found that radiation causes the appearance of complex defects, reducing the size of coherent scattering regions and the increase of the defect PL band.

DOI: 10.12693/APhysPolA.124.891

PACS: 61.80.–x, 78.55.Et, 71.55.Gs

1. Introduction

Zinc oxide is used as active component of heterojunction and electrode for thin film solar cells [1], piezoelectric transducers, transparent conductive films [2], light emission diodes [3] etc. The benefits of zinc oxide are low cost, large reserves of natural materials and high radiation resistance [4]. The latter makes ZnO one of the most promising materials suitable for use in high background radiation, for example, in outer space. For space-based applications, especially those in nearearth orbit, it is important to have radiation-resistant materials. In particular, the Van Allen belt contains high fluxes of electrons (0–10 MeV) and protons (10 MeV) [5].

Although high-quality bulk ZnO substrates are now under development, their high cost and limited availability currently preclude their use in mass production environments. Sapphire, on the other hand, is a relatively inexpensive substrate material and well suited for future production needs due to its low cost and high-crystalline perfection. ZnO can also be grown on sapphire epitaxially and with a high degree of surface flatness, an essential attribute for fabrication of devices [6].

Thus, the studies of changing a structure and optical properties in the radiation environment are important for space applications of devices based on ZnO. In this work, we report structural and optical properties of as-grown and electron irradiated ZnO films produced by direct current (DC) magnetron sputtering on sapphire substrates.

2. Experimental details

The ZnO films were deposited on Al_2O_3 (001) substrates at the temperature of 250 °C by direct current magnetron sputtering. A disc of zinc (100 mm in a diameter) with a purity of 99.99% was used as a target. High purity argon and oxygen gases were used as the sputtering and the reactive gas, respectively. The target-to-substrate distance was 40 mm. The chamber was pumped to a base pressure of 1×10^{-4} Pa before deposition. The films were grown in the ambient with Ar/O_2 ratio of 4:1. The dc power was maintained at 100 W. The deposition time was 90 min for all samples. The films were irradiated with 10 MeV electrons using the microtron electron accelerator M-30 at Institute of Electron Physics, NAS of Ukraine, Uzhgorod. The films were irradiated with the fluences of 10^{16} and 2×10^{16} ions/cm^2. During irradiation the samples were cooled by nitrogen vapor to −10 °C which controlled by copper–constantan thermocouple. The crystal structure of samples was studied by the X-ray diffraction (XRD) analysis where the Cu K_{α_1} radiation was used as a source ($\lambda = 0.154056$ nm). The XRD measurements were carried out by the DRON-4 Powder Diffraction system; a scan rate of 1°/min and a step size of 0.01° were used. It is important to note that the analyzed surface is about ≈ 1 cm^2 and the penetration depth of X-rays at 20–40 keV is a few μm. Measurement error of the peak position is about ±0.01° (2θ). Error of the c-lattice period determination is about ±0.0003 nm. The relative error in full width at half maximum (FWHM) calculations has been estimated to be ±2%. Room temperature photoluminescence (PL) spectra were measured with a Jobin–Yvon T64000 spectrometer equipped with a CCD detector, in a back scattering geometry, using the 325 nm excitation line of a He–Cd laser with an incident power of 10 mW.

3. Results and discussion

Figure 1 illustrates the θ–2θ XRD patterns of ZnO as-grown and irradiated films. They reveal a strong tex-

*corresponding author; e-mail: denysmyroniuk@gmail.com

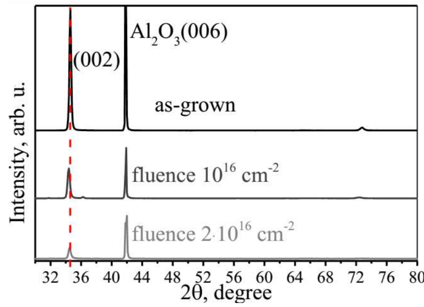

Fig. 1. XRD patterns of as-grown and electron irradiated ZnO films substrates.

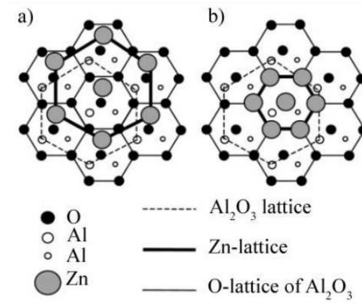

Fig. 3. Schematic diagram showing the epitaxial relationship of ZnO(001) grown on Al_2O_3(001) [6].

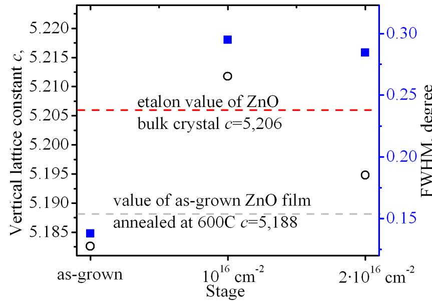

Fig. 2. The c lattice periods and FWHM values for (002) reflection of ZnO films.

turing along the [002] axis of wurtzite, lattice being the preferential orientation of films [7]. Other ZnO reflexes were absent in the full pattern. The reflex $\approx 41.5°$ relates to (006) plane of sapphire substrate.

In order to get more information about the electron irradiation effect on crystal structure, the values of lattice period c were calculated before and after the each irradiation. The c-lattice period was calculated from the Bragg equation as following [8]:

$$c = \frac{\lambda}{\sin \theta_{002}}.$$

Results are shown in Fig. 2.

Several factors affect the c value: (a) the lattice mismatch between sapphire substrate and ZnO film and (b) the difference between their coefficients of thermal expansion (CTE). The strain in films, which accumulates during film growth, often causes significant deterioration in terms of surface morphology, optical, and structural properties. Hence, the residual strain should itself be considered precisely to assess physical properties of the strained film.

The c surface of sapphire is composed of alternate layers of (sixfold symmetric) oxygen and (threefold symmetric) Al atoms, while in the wurtzite structure of ZnO, both O and Zn are sixfold symmetric about the ZnO c axis. In idealized case ZnO oxygen atoms would bond to the underlying sapphire Al atoms to form a structure (Fig. 3a) with a mismatch of 31.8% [6]. It is possible when the diffusion of atoms on the surface is suppressed at low growth temperatures. However, when the growth temperature is high, the kinetic energy of zinc atoms becomes high, and it is expected that the zinc atoms will become more diffused on the substrate surface. These effects cause zinc atoms to select sites having smaller lattice mismatch. In this case, a zinc atom is bounded to one oxygen atom in Al_2O_3, and a tetrahedral coordination of ZnO can be formed by supplying three other oxygen atoms. The relationships between the orientation of ZnO and substrate unit cells are 30°-twist (Fig. 3b). The oxygen sublattice has a lattice period of 2.75 Å, and the lattice mismatch to ZnO is -18.2% (compressive) [9].

It is worth to note that another strain due to CTE mismatch should be considered, especially for heteroepitaxy. Since there is a large difference between the growth and measurement temperatures, the CTE mismatch should have a large influence on lattice strain. As mentioned before, the strain due to CTE mismatch is revealed to be tensile (see CTE data for both Al_2O_3 and ZnO [10]).

As-grown film has the smaller c period (5.183 Å) than that of the ZnO bulk (5.206 Å), indicating the existence of a compressive stress along the c-axis or a tensile biaxial strain in the growth plane perpendicular to the c-axis. This tensile strain can be easily understood from the growth model given in Fig. 3a and considerations above. The existence of the strain also demonstrates that the film was being grown while keeping the epitaxial relationship with the substrate, which is an evidence of two--dimensional (2D) epitaxial growth [9].

After irradiation it was found that intensity and c value changed (Fig. 1, Fig. 2). In our case, there are several reasons, induced by electron irradiation, that may affect the (002) peak position and consequently lattice parameters: (i) electron–nucleus collisions which create defects and lead to swelling of the crystal lattice, (ii) electron–electron collisions lead to heating, i.e. radiation annealing and relaxation of the lattice. These factors are interrelated and counteracted between each other. Most of the energy losses in high-energy electron bombardment occur from electron–electron, rather than electron–nucleus, collisions [11]. Although the samples were cooled in nitrogen vapor, such e–e collisions lead to heating the microcrystals.

It was found that the electron irradiation by fluence 10^{16} cm^{-2} leads to the enlargement of the c-lattice parameter of ZnO film. It can be explained by creating defects. The increasing fluence to 2×10^{16} cm^{-2} causes the balance between the formation of defects and their annealing. As a result, the lattice of microcrystals can be relaxed (Fig. 2). This process also is reflected in the change of the FWHM values of corresponding reflexes (Fig. 2): irradiation by fluence 10^{16} cm^{-2} results in enhance of the FWHM, whereas fluence of 2×10^{16} cm^{-2} bring a slight decrease in the FWHM. The intensity of the (002) reflection keeps decreasing when the irradiation fluence increases.

The room temperature PL measurements were carried out to examine distribution of various emission levels observed in as-grown and irradiated with different fluences ZnO films, as shown in Fig. 4). The as-grown sample showed the intense near band edge (NBE) emission in ultraviolet (UV) region (≈ 3.24 eV) and weak deep-level emission orange region (≈ 2.1 eV); whereas, irradiated samples showed weaker UV emission and intense broad peak in orange-red (≈ 2 eV) region.

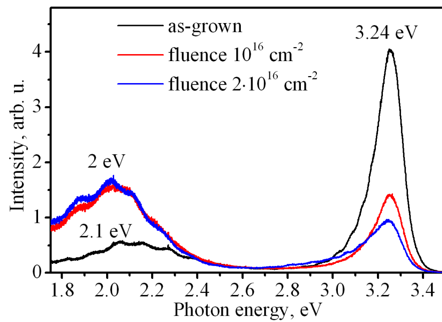

Fig. 4. PL spectra of as-grown and electron irradiated ZnO films substrates.

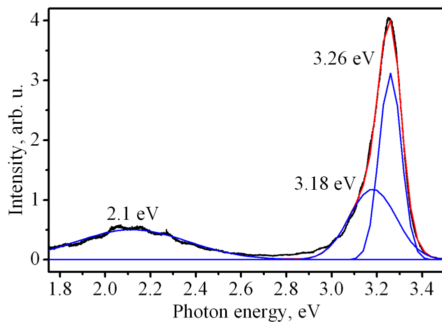

Fig. 5. Deconvolution of PL spectra of as-grown ZnO film.

The UV emission observed in as-grown ZnO films consists of intense band edge emission with a maximum at ≈ 3.26 eV and violet peak at ≈ 3.18 eV (Fig. 5). The first one is due to radiative recombination of localized excitons bound to neutral donor and/or acceptor [12]. Energy position of the PL band for unirradiated ZnO films shifted to low energy side by 100 meV in comparison with single-crystal zinc oxide (3.37 eV at 300 K [13]) due to elastic tensile strains. Against the background of the defect PL band recorded interference lines associated with the multiple reflection of radiation from the interface between film and substrate. The 3.18 eV peak in the violet region is due to band transition from the zinc interstitial (Zn_I) level to the valence band.

The NBE emissions were relatively broad due to overlap of the transitions corresponding to the free excitons as well as the excitons bound to neutral donors and acceptors. The deep level emission (DLE) in the orange-red region (2.1 eV) assigns to electronic transition between conduction band and deep acceptor oxygen interstitial (O_I) [14]. The orange-red emission from ZnO layers was explained by full potential linear muffin-tin orbital method, which suggested that the position of O_I level is located at 2.28 eV below the conduction band [15]. The broad width can be explained by set of transitions from conductive band and Zn_I level to O_I level.

After first step irradiation (fluence 10^{16} cm^{-2}) it clearly can be seen decreasing of NBE emission and arise of the DLE with center at ≈ 2 eV arises (Fig. 6). The intensity of UV luminescence (3.26 eV) decreases, which may be associated with an increase in density of the defect playing role of nonradiative recombination centers. Earlier, Look et al. have shown that electron irradiation with energy more than 1.6 MeV causes to create complex defects, which consist of the multiple displacements [11]. They proposed the idea of multiple displacements along a chain of atoms in ZnO. It was supposed that the electron energy is just high enough to displace a Zn atom. If the initial energy is higher (more than 1.6 MeV in our case), then the collision may give the Zn atom enough kinetic energy to knock out the O atom directly below it. This process can go on. Then the O atom can knock out the Zn below it, etc. At some point, the last knocked out Zn_I will be far enough from the parent V_{Zn} to avoid immediate recombination. On the other hand, the simple V_{Zn}–Zn_I (where V_{Zn} is zinc vacancy) Frenkel pair would be unstable, because the positively charged Zn_I must be more than a nearest neighbor distance away from the negatively charged V_{Zn} to avoid immediate recombination. If the chain defect suggested above is accurate, then an acceptor might be V_{Zn}–Zn_O–O_{Zn} (where Zn_O is zinc antisite and O_{Zn} is antisite of oxygen) and the donor, Zn_I.

A similar situation arises if the oxygen atoms were hit by the electrons. The complicated triple centre that contained associated V_{Zn}–Zn_O–O_{Zn} may be responsible for DLE band at 1.85 eV [16] (Fig. 4). Other DLE band at 2.2 eV can be associated with another acceptor defect complex, such as V_O–O_{Zn} (where V_O is oxygen vacancy) [17]. The increase in intensity at 2 eV indicates enhancement of the concentration of acceptor defects such as oxygen. At the same time, the low intensity of the Zn_I-related to emission band at 3.18 eV is caused by donor-acceptor pairs (DAP) transitions and relatively broad the DLE peaks are due to overlap of the emissions bands

related to transitions corresponding to the free excitons and Zn_I at room temperature [14, 18]. Indeed, radiative centres in n-type semiconductors are more likely acceptor-type defects.

In II–VI compounds, such as CdS, CdSe, ZnS and ZnSe centre responsible for self-activated emission was shown to be cation vacancy or DAP consisting of cation vacancy and shallow donor [19] and more complicated center that contained associated DAP and more distant donor was found [20].

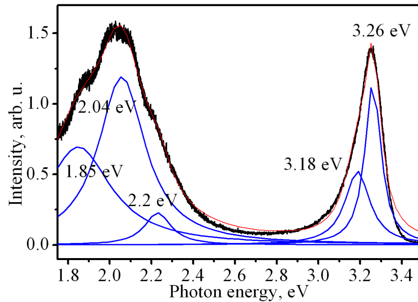

Fig. 6. Deconvolution of PL spectra of irradiated by fluence 10^{16} cm^{-2} ZnO film.

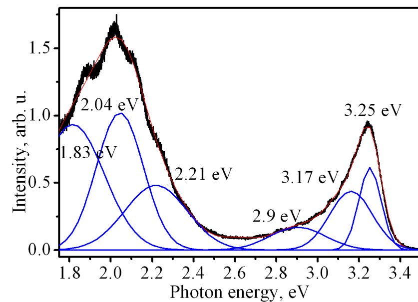

Fig. 7. Deconvolution of PL spectra of irradiated by fluence 2×10^{16} cm^{-2} ZnO film.

The proposed model is also confirmed by the absence of green (≈ 2.47 eV) and blue (≈ 2.9 eV) emission regions corresponding to oxygen [14, 21] and zinc vacancies [14], respectively. Thus mentioned form complexes with antisite defects. Figure 7 shows the deconvoluted PL spectra ZnO film irradiated by electrons with the 2×10^{16} cm^{-2} fluence. It is found further the decrease of NBE emission intensity and observed certain redistribution of peak intensities compared to the above results. In addition, there was revealed the appearance of the small shoulder of the peak at 2.9 eV which corresponded to transitions from conduction band and shallow donor level of Zn_I to acceptor level of V_{Zn}.

4. Conclusions

In summary, we have studied the effect of high energy electron irradiation on the structure and optical properties of ZnO thin films, grown by the dc magnetron sputtering. It was revealed that such type of irradiation significantly affects the structure, resulting in creation of the complex defects and radiation annealing. These findings were revealed from the analysis of the XRD and PL spectra. Furthermore, at the high irradiation fluences the films retain their lattice structure. Therefore, these films can be used in the optoelectronics devices in a high radiation background.

References

[1] W. Septina, S. Ikeda, T. Harada, M. Matsumura, *Phys. Status Solidi C* **1**, (2013).

[2] D.R. Sahu, S.-Y. Lin, J.-L. Huang, *Appl. Surf. Sci.* **252**, 7509 (2006).

[3] G.V. Lashkarev, V.A. Karpyna, V.I. Lazorenko, A.I. Ievtushenko, I.I. Shtepliuk, V.D. Khranovskyy, *Low Temp. Phys.* **37**, 226 (2011).

[4] D.C. Look, *Mater. Sci. Eng. B* **80**, 383 (2001).

[5] D.C. Look, D.C. Reynolds, J.W. Hemsky, *Appl. Phys. Lett.* **75**, 6 (1999).

[6] P. Fons, K. Iwata, A. Yamada, K. Matsubara, S. Niki, K. Nakahara, T. Tanabe, H. Takasu, *Appl. Phys. Lett.* **77**, 1801 (2000).

[7] N. Fujimura, T. Nishihara, S. Goto, J. Xu, T. Ito, *J. Cryst. Growth* **130**, 269 (1993).

[8] B.D. Cullity, *Wlements of X-ray Diffraction*, Addison-Wesley, 1956, p. 371.

[9] B.P. Zhang, K. Wakatsuki, N.T. Binh, N. Usami, Y. Segawa, *Thin Solid Films* **449**, 12 (2004).

[10] S.H. Park, T. Hanada, D.C. Oh, T. Minegishi, H. Goto, G. Fujimoto, J.S. Park, I.H. Im, J.H. Chang, M.W. Cho, T. Yao, K. Inaba, *Appl. Phys. Lett.* **91**, 231904 (2007).

[11] D.C. Look, J.W. Hemsky, J.R. Sizelove, *Phys. Rev. Lett.* **82**, 2552 (1999).

[12] Y.W. Chen, Y.C. Liu, S.X. Lu, et al., *J. Chem. Phys.* **123**, 134701 (2005).

[13] Ü. Özgür, Ya.I. Alivov, C. Liu, A. Teke, M.A. Reshchikov, S. Doğan, V. Avrutin, S.-J. Cho, H. Morkoç, *J. Appl. Phys.* **98**, 041301 (2005).

[14] C.H. Ahn, Y.Y. Kim, D.C. Kim, S.K. Mohanta, H.K. Cho, *J. Appl. Phys.* **105**, 013502 (2009).

[15] X.L. Wu, G.G. Siu, C.L. Fu, H.C. Ong, *Appl. Phys. Lett.* **78**, 2285 (2001).

[16] F. Tuomisto, K. Saarinen, D.C. Look, G.C. Farlow, *Phys. Rev. B* **72**, 085206 (2005).

[17] B. Lin, Z. Fu, Y. Jia, *Appl. Phys. Lett.* **79**, 943 (2001).

[18] N.O. Korsunska, L.V. Borkovska, B.M. Bulakh, L.Yu. Khomenkova, V.I. Kushnirenko, I.V. Markevich, *J. Lumin.* **102-103**, 733 (2003).

[19] G.D. Watkins, *Solid State Commun.* **12**, 589 (1973).

[20] J.R. James, J.E. Nicholls, B.C. Cavenett, J.J. Davies, D.J. Dunstan, *Solid State Commun.* **17**, 969 (1975).

[21] F.H. Leiter, H.R. Alves, A. Hofstaetter, D.M. Hoffmann, B.K. Meyer, *Phys. Status Solidi B* **226**, R4 (2001).